Indian Journal of Pure & Applied Physics
Vol. 52, December 2014, pp. 812-820

Dual solutions of three dimensional MHD boundary layer flow and heat transfer due to an axisymmetric shrinking sheet with viscous dissipation and heat generation/absorption

Dinesh Rajotia* & R N Jat

Department of Mathematics, University of Rajasthan, Jaipur 302 004, India

*E-mails: rajotia.dinesh@gmail.com & Khurkhuria_rnjat@yahoo.com

Received 23 September 2013; revised 10 March 2014; accepted 15 October 2014

An analysis is presented to study the effect of magnetic parameter on the certain range of suction parameter where the similarity solution exists of the three dimensional MHD boundary layer flow and heat transfer due to a porous axisymmetric shrinking sheet. The governing equations are transformed into self-similar non-linear ordinary differential equations by using suitable similarity transformations and then the transformed equations are solved numerically using a shooting method. The numerical results of velocity and temperature profiles as well as skin-friction coefficient and rate of heat transfer at the sheet are obtained and displayed graphically with different pertinent parameters to show interesting aspects of the solution. The investigation explores the conditions of the non-existence, the existence and duality of the similarity solutions which depend not only on the suction parameter S but magnetic parameter M also. The dual solutions exist in a certain domain of suction parameter S and an increment in the magnetic parameter M increases the domain of S where the solution exists. Also, the thickness of the momentum boundary layer and thermal boundary layer for the second solution are thicker than that of the first solution.

Keywords: Axisymmetric shrinking sheet, Boundary layer flow, Heat transfer, Suction, Magnetic effect, Dual solutions

1 Introduction

The viscous flow of an incompressible fluid over a stretching/shrinking sheet has many applications in manufacturing industries, such as glass-fiber production, wire drawing, paper production, extraction of polymer sheets and many others[1,2]. Crane[3] was the first who investigated the steady two dimensional flow over a linearly stretching sheet and found a closed form solution where the velocity on the boundary is away and proportional to the distance. The study of heat and mass transfer of the Crane's flow maintained at constant as well as variable wall temperature with suction was investigated by Gupta and Gupta[4]. Similarly, the work of Crane[3] was extended by Pavlov[5], Chakrabarti and Gupta[6], Carragher and Crane[7], Mukhopadhyay *et al*[8]., Mukhopadhyay and Anderson[9] and Jat *et al*[10]. under various physical conditions. Wang[11] studied the steady three dimensional flow of a viscous fluid over a plane surface which is stretched in its own plane in two lateral directions at different rates. Devi *et al*[12]., extended this problem to the unsteady three-dimensional boundary-layer flow. Further, Ariel[13] gave generalized three-dimensional flow due to a stretching sheet.

Recently, the development of an unusual flow due to a shrinking sheet has attracted considerable interest because the flow induced by the shrinking sheet shows quite distinct physical phenomena from the stretching sheet case. From consideration of continuity, Crane's[3] stretching sheet solution induces a far field suction towards the sheet, while flow over a shrinking sheet would give rise to a velocity away from the sheet. From a physical point of view, vorticity generated at the shrinking sheet is not confined within a boundary layer and a steady flow is not possible unless adequate suction is applied at the surface. Miklavcic and Wang[14] investigated both two-dimensional and axisymmetric viscous flow induced by a shrinking sheet in the presence of uniform suction and established the criteria of existence and uniqueness of the similarity solutions for both cases. Hayat *et al*[15]., reported the analytic solution of MHD flow of a second grade fluid over a shrinking sheet. While, analytic solution of MHD rotating flow by homotopy analysis method was again considered by Hayat *et al*[16]. Muhaimin *et al*[17]., investigated the effects of heat and mass transfer on nonlinear MHD boundary layer flow over a shrinking sheet in the presence of suction. The above problem of Miklavcic and Wang[14] was extended to power-law surface velocity by Fang[18]. Fang and Zhang[19] gave an exact solution of MHD boundary layer equations in the closed analytical form for the flow of an electrically conducting fluid in the presence of suction. Muhaimin *et al*[20]., investigated the effect of chemical reaction, heat and mass transfer on nonlinear MHD boundary layer past a porous shrinking sheet with suction. MHD viscous flow and heat transfer induced by a permeable shrinking sheet with prescribed surface heat flux is discussed by Ali *et al*[21]. He gave dual solutions for two dimensional flow and unique solution for axisymmetric flow. Bachok *et al*[22]., extended the idea of unsteady three dimensional boundary flow due to a permeable shrinking sheet and found dual solutions in a certain range of suction parameter and unsteadiness parameter. While, Bhattacharyya[23] reported boundary layer flow and heat transfer over an exponentially shrinking sheet. Wang[24] gave the stagnation flow towards a shrinking sheet and found that vorticity generated at the shrinking sheet can be confined within a boundary layer by stagnation flow as well. Effects of suction/blowing on steady boundary layer stagnation flow and heat transfer towards a shrinking sheet with thermal radiation was investigated by Bhattacharyya and Layek[25]. Further, Bhattacharyya *et al*[26]., gave the slip effects on boundary layer stagnation-point flow and heat transfer towards a shrinking sheet. Consequently, dual solutions in steady and unsteady stagnation-point flow over a shrinking sheet were given by Bhattacharyya[27,28]. Jat and Rajotia[29] investigated effects of variable thermal conductivity and variable Prandtl number on three dimensional MHD viscous flow and heat transfer due to a permeable axisymmetric shrinking sheet. Further, comparison between two dimensional and axisymmetric flow over to a permeable shrinking sheet with heat generation/absorption was considered by Jat and Rajotia[30].

Viscous dissipation and heat source/sink change the temperature distributions by playing a role like an energy source, which leads to affecting heat transfer rates. The merit of the effect of viscous dissipation and heat source/sink depends on whether the sheet is being stretching or shrinking. Consequently, effects of viscous dissipation and radiation on the thermal boundary layer over a non-linearly stretching sheet have been studied by Cortell[31]. Bhattacharyya[32] gave the effects of heat source/sink on MHD flow and heat transfer over a shrinking sheet with the suction/injunction. Such type of problems with the nanofluid has considerable useful and applicable aspects in the industry which were investigated by Hatami *et al*[33] and Hatami and Ganji[34, 35].

Miklavcic and Wang[14] reported the exact solution[33-35] for viscous flow induced by a shrinking sheet and found non-unique solutions for a certain range of suction parameter for both two dimensional and axisymmetric cases. Consequently, Ali *et al*[21]., investigated the above problem in the presence of the magnetic field and obtained dual solutions for the certain range of the suction parameter and magnetic parameter when the sheet shrinks in two dimensional while unique solution for axisymmetric flow. Therefore, in the present paper, the dual solutions of three dimensional MHD boundary layer flow and heat transfer of an electrically conducting fluid due to a porous axisymmetric shrinking sheet with viscous dissipation and heat source/sink, have been obtained.

2 Formulation of the Problem

Consider a three-dimensional MHD viscous incompressible flow of an electrically conducting fluid due to a porous axisymmetric shrinking sheet coincides with the plane z=0 and the flow is confined to z>0. The x and y axes are taken along the length and breadth of the sheet and z-axis is perpendicular to the sheet, respectively (Fig. 1). A constant magnetic field with strength B_0 is applied in the z-direction. The magnetic Reynolds number is taken to be small, so that the induced magnetic field is neglected and a suction is applied normal to sheet to contain the vorticity. All the other fluid properties are assumed constant throughout the motion.

Under the usual boundary layer approximations, the basic governing boundary layer equations with viscous dissipation and heat source/sink (Miklavcic & Wang[14] and Muhaimin *et al*[20].) are :

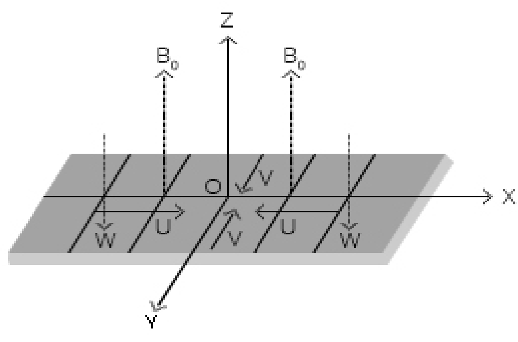

Fig. 1—Systematic diagram of physical model

$$\frac{\partial u}{\partial x}+\frac{\partial v}{\partial y}+\frac{\partial w}{\partial z}=0 \quad \ldots(1)$$

$$u\frac{\partial u}{\partial x}+v\frac{\partial u}{\partial y}+w\frac{\partial u}{\partial z}=-\frac{1}{\rho}\frac{\partial p}{\partial x}+\nu\left(\frac{\partial^2 u}{\partial z^2}\right)-\frac{\sigma B_0^{\,2}}{\rho}u \quad \ldots(2)$$

$$u\frac{\partial v}{\partial x}+v\frac{\partial v}{\partial y}+w\frac{\partial v}{\partial z}=-\frac{1}{\rho}\frac{\partial p}{\partial y}+\nu\left(\frac{\partial^2 v}{\partial z^2}\right)-\frac{\sigma B_0^{\,2}}{\rho}v \quad \ldots(3)$$

$$u\frac{\partial w}{\partial x}+v\frac{\partial w}{\partial y}+w\frac{\partial w}{\partial z}=-\frac{1}{\rho}\frac{\partial p}{\partial z}+\nu\left(\frac{\partial^2 w}{\partial z^2}\right) \quad \ldots(4)$$

$$u\frac{\partial T}{\partial x}+v\frac{\partial T}{\partial y}+w\frac{\partial T}{\partial z}=\frac{\kappa}{\rho c_p}\left(\frac{\partial^2 T}{\partial x^2}+\frac{\partial^2 T}{\partial y^2}+\frac{\partial^2 T}{\partial z^2}\right)$$
$$+\frac{\mu}{\rho c_p}\left[\begin{array}{l}2\left\{\left(\frac{\partial u}{\partial x}\right)^2+\left(\frac{\partial v}{\partial y}\right)^2+\left(\frac{\partial w}{\partial z}\right)^2\right\}+\\ \left(\frac{\partial u}{\partial y}+\frac{\partial v}{\partial x}\right)^2+\left(\frac{\partial u}{\partial z}+\frac{\partial w}{\partial x}\right)^2+\left(\frac{\partial v}{\partial z}+\frac{\partial w}{\partial y}\right)^2\end{array}\right]$$
$$+\frac{Q(T-T_\infty)}{\rho c_p} \quad \ldots(5)$$

where (u,v,w) be the velocity components along the (x,y,z) directions, respectively, p is the pressure, ρ the density of the fluid, μ the dynamic viscosity, $\nu=(\mu/\rho)$ the kinematic viscosity, σ the electrical conductivity, B_0 the magnetic induction, κ thermal conductivity, c_p the specific heat at constant pressure and Q is the volumetric rate of heat generation or absorption.

The boundary conditions applicable to the present flow are:

$$z=0:\ u=-U=-ax,\ \ v=-V=-ay,\ \ w=-W,$$
$$T=T_w \text{ and}$$
$$z\to\infty:\ u\to 0,\ \ v\to 0,\ \ T\to T_\infty \quad \ldots(6)$$

where a>0 is the shrinking constant, U and V are the shrinking velocities, W>0 is the suction velocity, T_w is the sheet temperature and T_∞ is the free stream temperature.

3 Analysis

Introducing the following similarity transformations:

$$u=axf'(\eta),\ \ v=ayf'(\eta),\ \ w=-2\sqrt{a\nu}\,f(\eta),$$
$$\theta(\eta)=\frac{T-T_\infty}{T_w-T_\infty} \text{ and } \eta=\sqrt{\frac{a}{\nu}}z \quad \ldots(7)$$

Eq. (1) is identically satisfied by the similarity transformations while Eq. (4) becomes:

$$\frac{p}{\rho}=\nu\frac{\partial w}{\partial z}-\frac{w^2}{2}+\text{Constant} \quad \ldots(8)$$

Eqs (2), (3) and (5) reduce to the Eqs (9) and (10) as:

$$f'''+2ff''-f'^2-Mf'=0 \quad \ldots(9)$$

$$\theta''+Pr\left[\begin{array}{l}2f\theta'+B\theta+12Ecf''\\+\left(Ec_x+Ec_y\right)f''^2\end{array}\right]=0 \quad \ldots(10)$$

Corresponding boundary conditions are:

$$\eta=0:\ f=S,\ f'=-1,\ \theta=1 \text{ and}$$
$$\eta\to\infty:\ f'\to 0,\ \theta\to 0 \quad \ldots(11)$$

where $S=\dfrac{W}{2\sqrt{a\nu}}$ is the suction parameter, $M=\dfrac{\sigma B_0^{\,2}}{\rho a}$ is the magnetic parameter, $Pr=\dfrac{\mu c_p}{\kappa}$ is the Prandtl number, $B=\dfrac{Q}{a\rho c_p}$ is the Heat Source $(B>0)$ or Sink $(B<0)$ parameter, $Ec=\dfrac{\mu a}{\rho c_p(T_w-T_\infty)}$ is the Eckert number, $Ec_x=\dfrac{a^2x^2}{c_p(T_w-T_\infty)}$ and $Ec_y=\dfrac{a^2y^2}{c_p(T_w-T_\infty)}$ are the local Eckert numbers based on the variables x and y, respectively.

The physical quantity of interest is the local skin friction coefficient C_f on the surface along the x and y directions, which are denoted by C_{fx} and C_{fy}, respectively and the local Nusselt number Nu i.e. surface heat transfer are given by:

$$C_{fx}=\frac{\tau_{wx}}{\rho U^2/2}=\frac{\mu\left(\frac{\partial u}{\partial z}\right)_{z=0}}{\rho U^2/2}=\frac{2}{\sqrt{\mathrm{Re}_x}}f''(0)$$

$$C_{fy}=\frac{\tau_{wy}}{\rho V^2/2}=\frac{\mu\left(\frac{\partial v}{\partial z}\right)_{z=0}}{\rho V^2/2}=\frac{2}{\sqrt{\mathrm{Re}_y}}f''(0)$$

and

$$Nu = -\frac{x\left(\frac{\partial T}{\partial z}\right)_{z=0}}{\left(T_w - T_\infty\right)} = -\sqrt{\mathrm{Re}_x}\,\theta'(0) \qquad \ldots(12)$$

where τ_{wx} and τ_{wy} are the wall shear stresses along the x and y directions, respectively and $\mathrm{Re}_x = \frac{Ux}{\nu}$ and $\mathrm{Re}_y = \frac{Vy}{\nu}$ are the local Reynolds numbers.

4 Method of Solution

The set of nonlinear ordinary differential Eqs (9) and (10) with boundary conditions given in Eq. (11) are solved numerically by converting them to an initial value problem (IVP). We set:

$$\begin{aligned} f' &= z \\ z' &= p \\ p' &= -2fp + z^2 + Mz \end{aligned} \qquad \ldots(13)$$

$$\begin{aligned} \theta' &= q \\ q' &= -\mathrm{Pr}\begin{bmatrix} 2fq + B.\theta + 12Ec.z^2 \\ +(Ec_x + Ec_y)p^2 \end{bmatrix} \end{aligned} \qquad \ldots(14)$$

With boundary conditions:

$$f(0) = S\,,\; f'(0) = -1\,,\; \theta(0) = 1\,,$$
$$f'(\eta_\infty) = 0 \text{ and } \theta(\eta_\infty) = 0 \qquad \ldots(15)$$

In order to integrate Eqs (13) and (14) as an initial value problem, one requires a value for $p(0)$ i.e. $f''(0)$ and $q(0)$ i.e. $\theta'(0)$ but no such values are given in the boundary conditions. The suitable guesses for $f''(0)$ and $\theta'(0)$ are chosen by the shooting technique and the fourth order Runge – Kutta method is applied to obtain the solution. Then we compare the calculated values for f' and θ at $\eta_\infty = 8$ (say) with the given boundary conditions $f'(8)=0$ and $\theta(0)=0$ and adjust the estimated values of $f''(0)$ and $\theta'(0)$ using the Secant method to give a better approximation for the solution. The step-size is taken as $h = 0.001$. The above procedure is repeated until we get the converged results within a tolerance limit of 10^{-7}. All the computations are done in the Matlab software which uses a symbolic and computational language.

5 Results and Discussion

The numerical computation has been carried out for obtaining the condition under which the steady flow is possible over the axisymmetric shrinking sheet for various values of the parameters involved such as suction parameter S, magnetic parameter M, Prandtl number Pr, heat source/sink parameter B and Eckert number Ec and local Eckert numbers Ec_x and Ec_y.

First of all, Miklavcic and Wang[14] studied the exact solution of the boundary layer flow over an axisymmetric shrinking sheet in the presence of uniform suction without magnetic field i.e. M=0 and obtained that the existence of the dual solution depends on a certain range of the suction parameter S only and he found that the similarity solution exists for $S \geq S_0$=1.3117586 and there is no solution for $S<S_0$. In the present analysis, the dual solutions of boundary layer flow without the magnetic field exist for $S \geq 1.312$ (likely equal to S_0) and consequently, there is no similarity solution for S<1.312. This gives us a favourable agreement with the solution of Miklavcic and Wang[14].

Consequently, further investigation of the dual solutions is carried out in the presence of the magnetic field over the axisymmetric shrinking sheet with uniform suction. The analysis shows that the existence of the dual solution depends not only on the suction parameter S but on the magnetic parameter M as well. Fig. 2 shows the skin friction coefficient against suction parameter S for several values of M. It is observed that the domain of S, where the dual solutions exist is increased with increasing values of M. The magnetic parameter delays the boundary layer

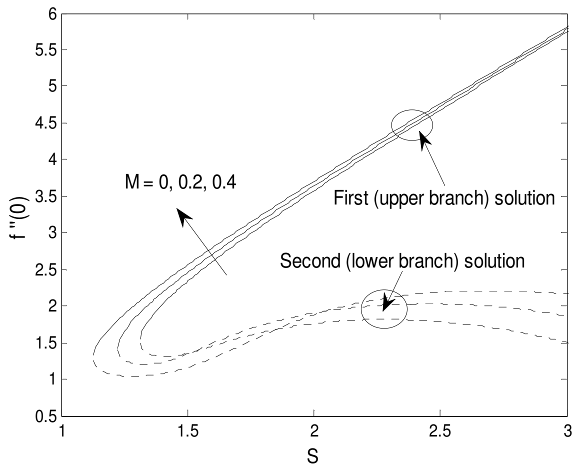

Fig. 2 — Skin friction coefficient against S with several values of magnetic parameter M

separation from the surface. Also, for increasing values of S, the skin friction coefficient $f''(0)$ increases for the first solution (upper branch) while for the second solution (lower branch) it initially decreases slightly then increases and again for higher values of S it slightly decreases. Further, for increasing values of M, $f''(0)$ increases for the first solution, while for the second solution, initially it decreases and for larger values of S, it starts to increase again with M. Thus, for dual similarity solutions, the first solution is stable while the second one is unstable.

Moreover, the particular values of domain of S where the dual similarity solutions exist with various values of M are given in Table 1. It is observed that for M=0.5, the domain of the dual similarity solution becomes S≥1.07 i.e. be wider than S≥1.312 at M=0.

Dual velocity profile $f'(\eta)$ for various values of magnetic parameter $M$is shown in Fig. 3 and it is found that with increasing values of M, the velocity profile increases in the first solution case while decreases in the second solution case, although as compared to the diminution of velocity for the second solution the velocity enhancement in the first solution is small. Also, in the first solution case the decrement in the momentum boundary layer thickness with M is happening due to the Lorentz force created by M which slows the fluid flow. Figure 4 shows the effect of suction parameter on the velocity profile. It is found from Fig. 4 that the dimensionless velocity profile $f'(\eta)$ increases with the increasing value of S for the first solution while for the second solution it decreases with increasing of S. Furthermore, it is evident to say that in every case of dual solutions of the velocity profile, the momentum boundary layer thickness for the second solution is larger than that of the first solution.

Dual temperature profile for various values of M and S is shown in Figs 5 and 6, respectively. Figure 5 shows that with increasing values of M, the temperature profile as well as thermal boundary layer thickness decrease for the first solution while increase very quickly for the second solution. Here, it is very important to conclude that M affects the second solution very much in comparison to the first solution. Figure 6 shows that temperature at a point decreases with the increasing value of S for the first solution while for the second solution it increases with S. Furthermore, it is very important to note that the temperature profiles with M and S likely just give reverse phenomena in comparison with that of the velocity profiles.

Table 1 — Range of S for existence of the dual solutions with several values of M

Magnetic parameter M	Dual solutions (First and Second)
0	$S \geq 1.312$
0.05	$S \geq 1.291$
0.1	$S \geq 1.269$
0.15	$S \geq 1.246$
0.2	$S \geq 1.223$
0.3	$S \geq 1.176$
0.4	$S \geq 1.125$
0.5	$S \geq 1.07$

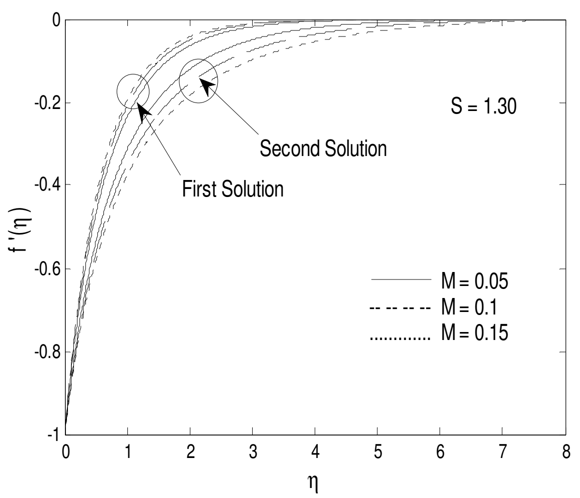

Fig. 3 — Dual velocity profile for various values of M

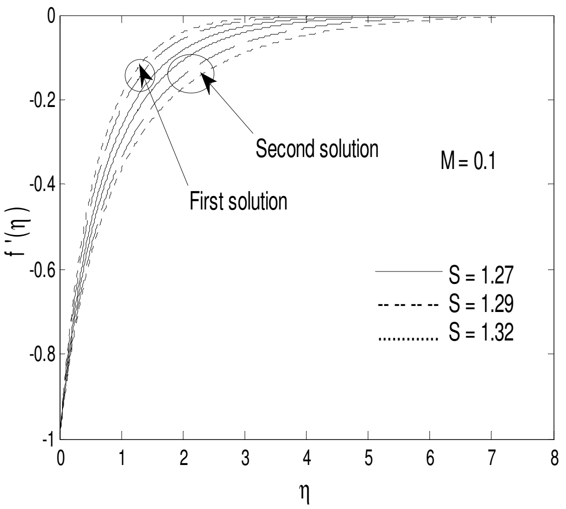

Fig. 4 — Dual velocity profile for various values of S

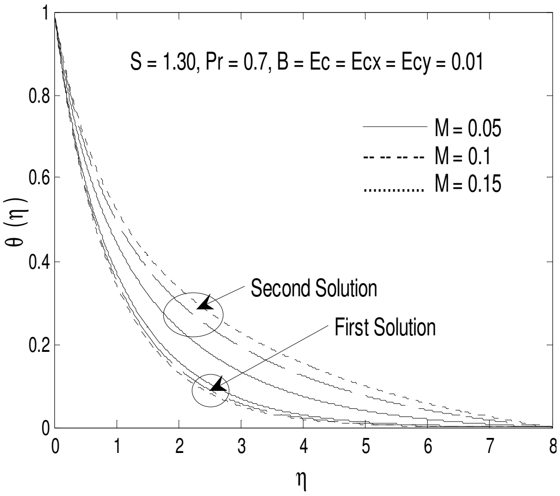

Fig. 5 — Dual temperature profile for various values of *M*

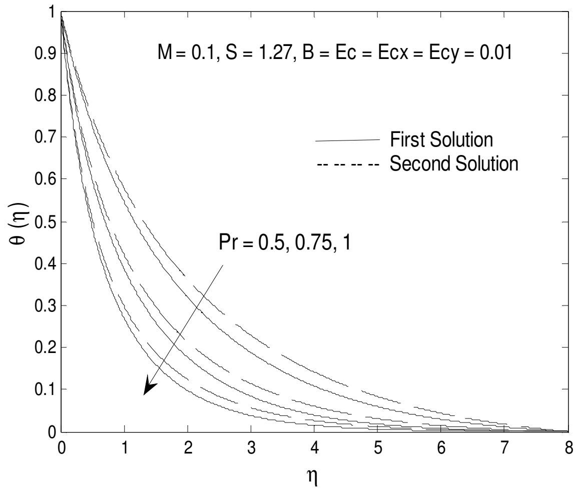

Fig. 7 — Dual temperature profile for various values of *Pr*

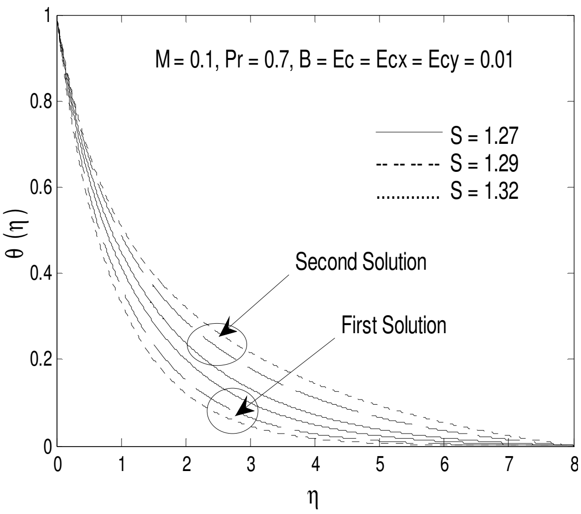

Fig. 6 — Dual temperature profile for various values of *S*

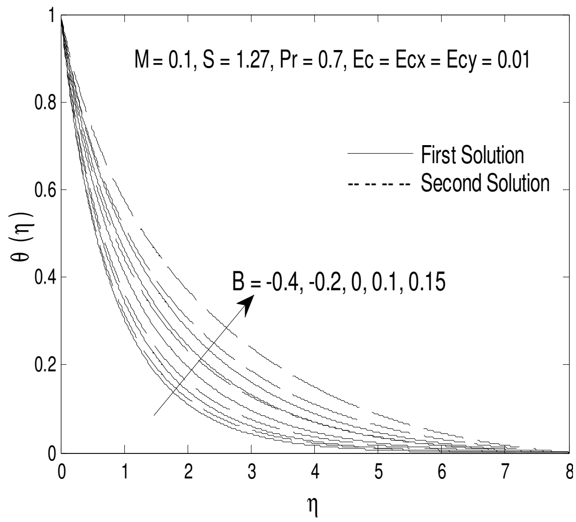

Fig .8 — Dual temperature profile for various values of *B*

The dual temperature profile for various values of *Pr* with a magnetic field is shown in Fig. 7. It is observed that in the presence of the magnetic field, the thermal boundary layer thickness of both first and second solutions reduces significantly due to increase of *Pr*. Since the Prandtl number is inversely proportional to the thermal conductivity, thus the fluids with the lower *Pr* have higher thermal conductivities and consequently the heat diffusion is faster in this case. On the other hand, for higher *Pr* fluids the heat diffusion slows down. The effects of heat source/sink *B* on dual temperature profile is shown in Fig. 8. It finds that the temperature of the fluid as well as the thermal boundary layer thickness for both cases decrease for the increasing strength in heat sink $B < 0$ but due to increase in strength of heat source $B > 0$ the temperature profile for both solutions increases.

Dual temperature profile with several values of Eckert number *Ec* is shown in Fig. 9. It is observed from Fig. 9 that with increasing values of *Ec* the temperature profiles increase in both cases and this happens due to the fact that viscous dissipation creates frictional heating which is stored in the fluid as heat energy and this heat energy increases the thickness of the thermal boundary layer as a result. Finally, the effects of local Eckert numbers Ec_x and Ec_y on dual temperature profiles are shown in Figs 10 and 11, respectively. It is noticed that the temperature profile for both cases increase with

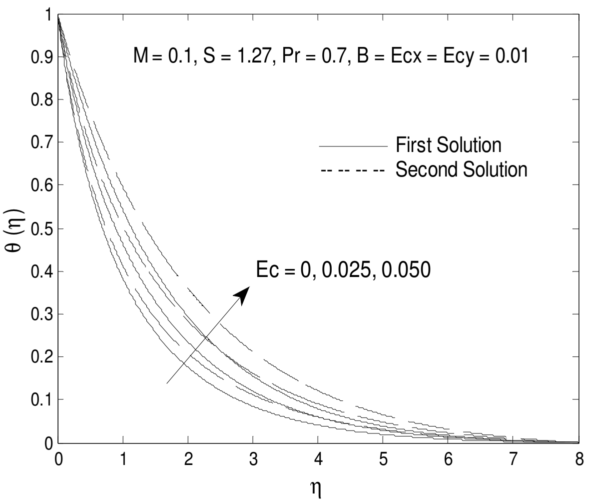

Fig. 9 — Dual temperature profile for various values of *Ec*

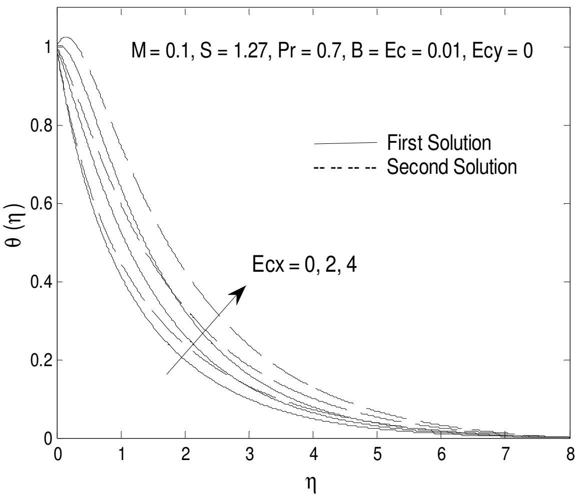

Fig. 10 — Dual temperature profile for various values of Ec_x

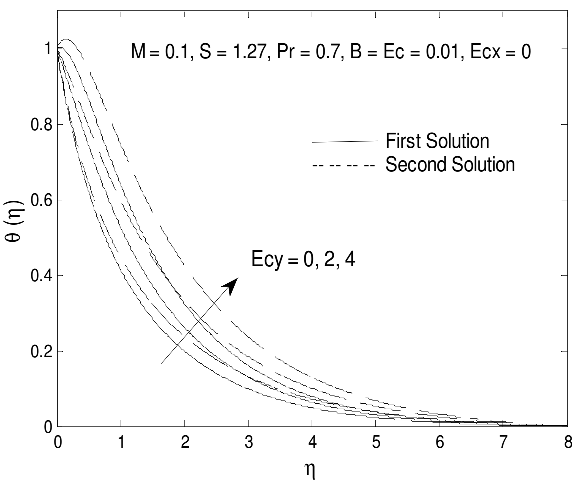

Fig. 11 — Dual temperature profile for various values of Ec_y

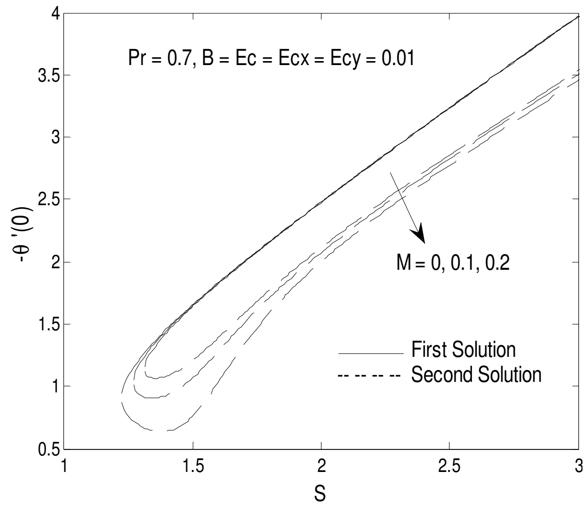

Fig. 12 — Dual temperature gradient at the sheet $-\theta'(0)$ with *S* for various values of *M*

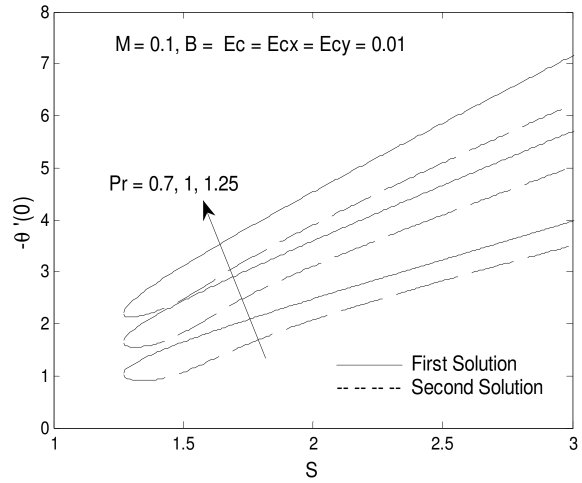

Fig. 13 — Dual temperature gradient at the sheet $-\theta'(0)$ with *S* for various values of *Pr*

increasing values of Ec_x as well as Ec_y. However, similar to the velocity field, it is evident to say that in all prescribed cases the thermal boundary layer thickness for the second solution is thicker than that of the first solution.

Analysis of the dual nature of the temperature gradient $-\theta'(0)$ at the sheet (i.e. rate of heat transfer from the surface to the fluid) against *S* for various values of different parameters involving such as *M*, *Pr*, *B* and *Ec* are given in Figs 12-15, respectively. It is observed from Fig. 12 that in the case of the first solution, the rate of heat transfer at the sheet $-\theta'(0)$ increases very slightly with increasing of *M* in a certain range of small values of *S*, whereas it

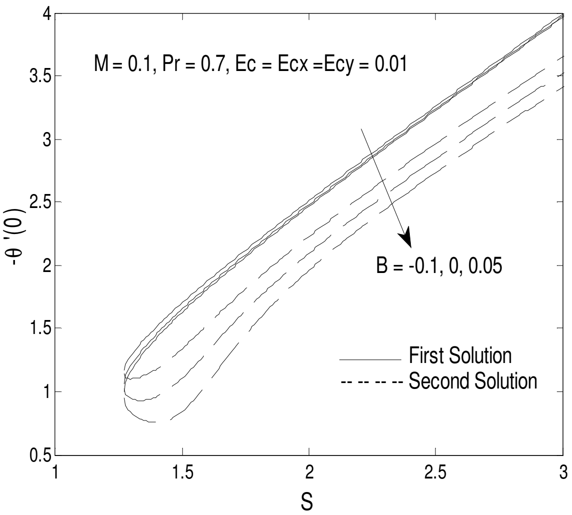

Fig. 14 — Dual temperature gradient at the sheet $-\theta'(0)$ with S for various values of B

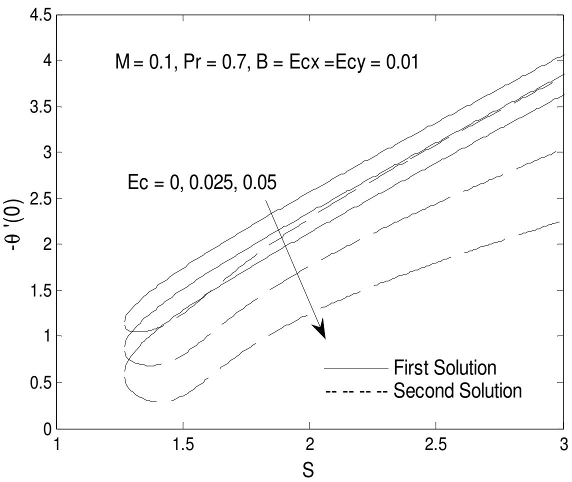

Fig. 15 — Dual temperature gradient at the sheet $-\theta'(0)$ with S for various values of Ec

decreases with M for the second solution case. Figure 13 shows that for increasing values of Pr, $-\theta'(0)$ increases for both solutions. From Figs 14 and 15, it is noticed that for both solutions the rate of heat transfer at the surface decreases with increasing values of B and Ec. Consequently, from Figs 12-15, it is found that the rate of heat transfer at the sheet increases with increasing values of S in both cases of first and second solutions.

6 Conclusions

The effect of the magnetic parameter on the dual character of the similarity solution of three dimensional MHD boundary layer flow and heat transfer over a porous axisymmetric shrinking sheet in the presence of uniform suction has been investigated. The similarity equations are obtained and solved numerically by the shooting method. The study reveals that the dual solutions are possible only in a certain range of the suction parameter which can be increased by the magnetic parameter. Moreover, for the first solution the velocity increases with suction and magnetic parameters while decreases for the second solution. While an opposite behaviour is observed in the temperature profile for both solutions with suction and magnetic parameters in comparison with that of the velocity profile. The study suggests that the thickness of the momentum boundary layer and thermal boundary layer for the second solution is thicker than that of the first solution. The skin friction coefficient for the first solution increases with increasing values of suction parameter and magnetic parameter both but for the second solution it gives fluctuating nature. The rate of heat transfer at the sheet decreases for increasing of Eckert number and heat source/sink parameter while increases with Prandtl number and suction parameter for both cases but for increasing of magnetic parameter, it increases for the first solution while decreases for the second solution.

Acknowledgement

This work has been carried out with the financial support of CSIR, India in the form of Senior Research Fellowship (SRF) under research scheme no. 09/149(0593) /2011-EMR-I awarded to one of the authors (Dinesh Rajotia).

References

1 Fisher E G, *New York Wiley*, (1976).
2 Atlan T, Oh S & Gegrl H, *American Society of Metals*, (1979).
3 Crane L J, *Z Angew Math Phys,* 21(4) (1970) 645.
4 Gupta P S & Gupta A S, *Canadian J of Chemical Engineering*, 55 (1977) 744.
5 Pavlov K B, *Magnitnaya Gidrodinamika*, 4 (1974) 146.
6 Chakrabarti A C & Gupta A S, *Quarterly of Appl Mathematics* 37 (1979) 73.
7 Carragher P & Crane L J, *Zeitschrift fur Angewandte Mathematik und Mechanik,* 62 (1982) 564.
8 Mukhopadhyay S, Layek G C & Samad S A, *Int J of Heat & Mass Transfer,* 48 (2005) 4460.
9 Mukhopadhyay S & Andersson H I, *Heat Mass Transfer,* 45 (2009) 1447.
10 Jat R N, Saxena V & Rajotia D, *Indian J of Pure & Appl Phys*, 51 (2013) 683.
11 Wang C Y, *Phys Fluids,* 27(8) (1984) 1915.
12 Devi S, Takhar H S & Nath G, *Int J of Heat & Mass Transfer,* 29(12) (1986) 1996.

13 Ariel P D, *ZAMM,* 83(12) (2003) 844.
14 Miklavcic M & Wang C Y, *Quarterly Appl Mathematics*, 64 (2006) 283.
15 Hayat T, Abbas Z & Sajid M, *J of Appl Mechanics,* 74 (2007) 1165.
16 Hayat T, Sajid M & Javed T, *Nonlinear Dynamics,* 51 (2008) 259.
17 Muhaimin, Kandasamy R & Khamis A B, *Appl Mathematics & Mechanics*, 29(10) (2008) 1309.
18 Fang T, *Int J of Heat & Mass Transfer*, 51 (2008) 5838.
19 Fang T & Zhang J, *Communi in Nonlinear Sci & Numerical Simula*, 14 (2009) 2853.
20 Muhaimin, Kandasamy R, Hashim I & Khamis A B, *Theoret Appl Mech*, 36(2) (2009) 101.
21 Ali F M, Nazar R & Arifin N M, *Wseas Trans on Mathematics*, 5(9) (2010) 365.
22 Bachok N, Ishak A & Pop I, *Appl Mathematics & Mechanics*, 31(11) (2010) 1421.
23 Bhattacharyya K, *Chinese Phys Lett*, 28(7) (2011) 074701.
24 Wang C Y, *Int J of Non-Linear Mechanics*, 43 (2008) 377.
25 Bhattacharyya K & Layek G C, *Int J of Heat & Mass Transfer*, 54 (2011) 302.
26 Bhattacharyya K, Mukhopadhyay S & Layek G C, *Int J of Heat & Mass Transfer*, 54 (2011) 308.
27 Bhattacharyya K, *Int Communi in Heat & Mass Transfer*, 38(7) (2011) 917.
28 Bhattacharyya K, *Chinese Phys Lett*, 28(8) (2011) 084702.
29 Jat R N & Rajotia D, *Int J of Energy & Tech,* 6 (1) (2014) 1.
30 Jat R N & Rajotia D, *Indian J of Pure & Appl Phys*, 52 (2014).
31 Cortell R, *Phys Letters*, 372(5) (2008) 631.
32 Bhattacharyya K, *Chemical Engi Res Bulletin*, 15(1) (2011) 12.
33 M Hatami, A Hasanpour & D D Ganji, *Energy Conversion & Management,* 74 (2013) 9.
34 Hatami M & Ganji D D, *J of Molecular Liquids*, 1 (2014) 159.
35 Hatami M & Ganji D D, *Energy Conversion & Management,* 78 (2014) 347